Oxygenation of the ocean and sediments: Consequences for the seafloor carbonate factory

J.A. Higgins [a,*], W.W. Fischer [b], D.P. Schrag [a]

[a] Department of Earth and Planetary Science, Harvard University, 20 Oxford Street, Cambridge, MA 02138, United States
[b] Division of Geological and Planetary Science, California Institute of Technology, 1200 E. California Boulevard, Pasadena, CA 91125, United States

ARTICLE INFO

ABSTRACT

Observed changes in the source of CaCO$_3$ sediments since Archean time suggest a first order pattern of decreasing abundance of carbonate cements precipitated directly on the seafloor. We propose that the observed reduction in CaCO$_3$ precipitation on the seafloor is caused by a decrease in CaCO$_3$ saturation in sediments related to increased oxic cycling of organic carbon and a decline in the size of the marine DIC reservoir. Using a simple model of CaCO$_3$ saturation in the ocean, we show that changes in ocean–atmosphere redox and the size of the marine carbon reservoir strongly influence the ability of sediments to dissolve or precipitate CaCO$_3$. Oxic oceans like the modern are characterized by large gradients in CaCO$_3$ saturation. Calcium carbonate precipitates where CaCO$_3$ saturation is high (surface ocean) and dissolves where CaCO$_3$ saturation is low (sediments). In contrast, anoxic respiration of organic carbon and/or a large ocean carbon reservoir leads to a more homogeneous distribution of CaCO$_3$ saturation in the ocean and sediments. This effect suppresses CaCO$_3$ dissolution and promotes CaCO$_3$ precipitation on the seafloor. Our results suggest that the growth or contraction of gradients in CaCO$_3$ saturation in the ocean and sediments may explain the observed trends in carbonate precipitation on the seafloor in the Precambrian and changes in the global CaCO$_3$ cycle, such as the reappearance of seafloor precipitates and the drowning of carbonate platforms during episodes of widespread anoxia in the Phanerozoic marine basins. Our work provides novel insights into the consequences of the long-term geochemical evolution of the ocean and atmosphere for the global CaCO$_3$ cycle.

© 2009 Published by Elsevier B.V.

1. Introduction

The abundance of carbonate minerals in marine sedimentary rocks since 3.43 Ga (Allwood et al., 2006) suggests that precipitation of CaCO$_3$ has been an important sink of alkalinity and CO$_2$ over much of Earth history. Reconstructions of ancient and modern carbonate depositional systems indicate that the large-scale features of shallow-water carbonate sedimentation (paleogeography, platform architecture, and sequence stratigraphy; Grotzinger and James, 2000) have changed little over the last 3 billion yrs, suggesting similar controls on global patterns of CaCO$_3$ deposition (e.g. climate, weathering, sedimentary accommodation and accumulation). Importantly, the continuity of CaCO$_3$ deposition has been maintained in spite of large changes in the sources of carbonate sediment in shelf and slope environments over Earth history. During Archean and Paleoproterozoic time, significant CaCO$_3$ precipitation occurred directly on (and in) the seafloor as crystal fans, microdigitate stromatolites, and isopachous cements (Grotzinger and Reed, 1983; Kah and Grotzinger, 1992; Sumner and Grotzinger, 1996a, 2000; Grotzinger and James, 2000;). Seafloor precipitates declined during the Meso- and Neoproterozoic in favor of carbonate muds (micrite) and trap-and-bind stromatolites (Grotzinger, 1990; Grotzinger and James,

2000). In latest Edicaran seas, CaCO$_3$-producing eukaryotes evolved (Grotzinger et al., 1995). Since Cambrian–Ordovician time, carbonate sediments have been composed primarily of skeletal CaCO$_3$, with the exception of brief (millions of years) intervals associated with anoxia and mass extinction (Grotzinger and Knoll, 1995; Copper, 2002; Pruss et al., 2006; Knoll et al., 2007) where authigenic seafloor precipitates return as a conspicuous CaCO$_3$ sink.

In this paper we try to understand changes in the source and cycling of CaCO$_3$ in the ocean over Earth history in the context of changes in pCO$_2$, pO$_2$, and ocean chemistry. We do this by considering the processes that control the distribution of CaCO$_3$ saturation in seawater and sediments, defined as

$$\Omega = \frac{\gamma Ca^{2+} \cdot \gamma CO_3^{2-}}{K_{sp}} \qquad (1)$$

where γCa^{2+} and γCO_3^{2-} are the activities of Ca^{2+} and CO$_3^{2-}$ in seawater (Garrels et al., 1961) and K_{sp} is the thermodynamic solubility constant for CaCO$_3$ (calcite for simplicity). As long as [Ca^{2+}]>>[CO$_3^{2-}$], Ω is related to the parameter ΔCO_3^{2-} used in chemical oceanography in that $\Omega = \Delta CO_3^{2-} / CO_3^{2-}(sat) + 1$ where CO$_3^{2-}$(sat) is the concentration of carbonate ion at calcite saturation (i.e. CO$_3^{2-}$(sat) $= K_{sp} / Ca^{2+}$). In the following section, we examine the factors that control carbonate

* Corresponding author. Tel.: +1 617 852 9931.
   E-mail address: jhiggins@fas.harvard.edu (J.A. Higgins).

saturation (Ω) in seawater on geologic timescales. We then develop a simple model of the global $CaCO_3$ cycle that takes into account the effect of gradients in Ω in the ocean and sediments and use the model to explore how secular changes in pO_2, pCO_2, and ocean chemistry affect the locus of precipitation and the rate of $CaCO_3$ dissolution. Our results indicate that under oxic conditions, like those found in modern ocean basins, the production and respiration of organic carbon creates large gradients in Ω between (and within) the water column and sediments, leading to a supersaturated surface ocean and undersaturation in sediments at all depths. In contrast, in an ocean that is more reducing and/or contains large amounts of dissolved inorganic carbon, a more homogeneous distribution of Ω in the ocean and sediments is expected. A more homogenous distribution of Ω will tend to suppress $CaCO_3$ dissolution and promote $CaCO_3$ precipitation on the seafloor. Finally, we discuss implications of the model for observed changes in the source and cycling of $CaCO_3$ over Earth history.

2. What controls the average value of Ω in seawater on geologic timescales?

Feedbacks between volcanic outgassing of CO_2, weathering of silicate minerals, and the burial of carbonates in the ocean are thought to control the global carbon cycle and climate on geologic timescales (Urey, 1952; Walker et al., 1981). The reaction of carbonic acid with silicate rocks adds alkalinity to seawater, shifting the partitioning of carbon species towards CO_3^{2-} and higher values of Ω. As long as silicate weathering continues to deliver alkalinity to the oceans, Ω will increase until carbonate minerals precipitate and the burial of $CaCO_3$ balances the flux of alkalinity from weathering (Walker et al., 1981). It is important to note that the balance between $CaCO_3$ burial and alkalinity inputs does not imply a particular value of Ω in the ocean. Rather, the average value of Ω in the ocean will reflect the dynamic balance between Ca^{2+}, CO_3^{2-}, and the solubility of $CaCO_3$ (K_{sp}):

$$\frac{d\Omega}{dt} = \frac{d}{dt}\left(\frac{\gamma_{Ca}Ca^{2+} \cdot \gamma_{CO3}CO_3^{2-}}{K_{sp}}\right). \tag{2}$$

Eq. (2) can be simplified if we limit ourselves to short timescales (~10^4 yrs) and treat as constant those variables with characteristic timescales $>10^6$ yrs; these include: Ca^{2+} (Martin and Meybeck, 1979), ion activity coefficients (γ_{Ca} and γ_{CO3} are functions of the major element composition of seawater, especially Mg^{2+} and SO_4^{2-}, both of which have residence times of $>10^7$ yrs; (Garrels et al., 1961)), and K_{sp} (Mg/Ca in seawater is thought to influence primary carbonate mineralogy; (Stanley and Hardie, 1998)). Shorter timescale changes in K_{sp}, for example due to variations in ocean temperature, are small and can be neglected. What is left is an equation for the average value of Ω in seawater over time that depends primarily on changes in CO_3^{2-}. The concentration of CO_3^{2-} in seawater depends, in turn, on the sum of dissolved inorganic carbon species ($DIC = CO_2 + HCO_3^- + CO_3^{2-}$), the sum of dissolved species of weak acids/bases other than CO_2 (e.g. H_2S), and alkalinity ($ALK = \sum$ strong base cations $- \sum$ strong acid anions). Since the residence time carbon in the ocean is much longer than the timescales for adjustment in seawater alkalinity ($>10^5$ vs. ~10^4 yrs; (Walker et al., 1981; Archer et al., 1997), Eq. (2) can be further reduced to a simple function of alkalinity:

$$\frac{d\Omega}{dt} \propto \frac{dCO_3^{2-}}{dt} \propto \frac{dALK}{dt}. \tag{3}$$

This result demonstrates that, on timescales of ~10^4 yrs the average value of Ω in seawater is strongly tied to the global alkalinity cycle. The global alkalinity cycle reflects the balance between alkalinity sources (weathering and sedimentary $CaCO_3$ dissolution) and sinks ($CaCO_3$ precipitation). Importantly, thermodynamic considerations and experimental studies of both biogenic $CaCO_3$

precipitation (Gattuso et al., 1998; Langdon et al., 2000; Riebesell et al., 2000; Broecker et al., 2001) and inorganic $CaCO_3$ precipitation/ dissolution (Burton and Walter, 1987; Zhong and Mucci, 1989; Zuddas and Mucci, 1998; Morse et al., 2007) indicate that rates of precipitation and dissolution depend on the local value of Ω. Because precipitation and dissolution rates depend on local values of Ω, the distribution of Ω within the ocean and sediments will play an important role in determining where precipitation and dissolution are likely to occur and how the average value of Ω in the ocean is controlled on geologic timescales.

3. A simple model of the global $CaCO_3$ cycle

In this section, we develop a simple model of the global $CaCO_3$ cycle to understand how gradients in Ω within the ocean and sediments affect the locus of precipitation and importance of dissolution. Our model is based on a simple differential equation for alkalinity in seawater and includes weathering (W), $CaCO_3$ precipitation (P), and $CaCO_3$ dissolution (D):

$$\frac{dALK}{dt} = W - P + D. \tag{4}$$

We use rate equations for $CaCO_3$ precipitation and dissolution that are similar to previous global modeling studies (Zeebe and Westbroek, 2003; Ridgwell, 2005) and based on inorganic precipitation/dissolution experiments (Morse, 1978; Mucci and Morse, 1983):

$$P = k_p \cdot \left(\Omega_p - 1\right)^{n_p} \tag{5a}$$

$$D = k_d \cdot (1 - \Omega_d)^{n_d} \tag{5b}$$

where Ω_p and Ω_d are the local values of $CaCO_3$ saturation, k_p and k_d are the reaction rate constants, and n_p and n_d are the reaction orders for $CaCO_3$ precipitation and dissolution, respectively. We assume all reactions are second-order ($n = 2$) for simplicity; different values do not significantly change our results. Because global rates of $CaCO_3$ precipitation and dissolution reflect contributions from a range of $CaCO_3$ sources (e.g. corals, algae, inorganic cements) and environments (e.g. continental shelf vs. deep sea), we treat $CaCO_3$ cycling in the ocean as the sum of individual precipitation/dissolution terms:

$$\frac{dALK}{dt} = W - \sum_{i=1}^{j} k_p(i) \cdot \left(\Omega_p(i) - 1\right)^2 + \sum_{x=1}^{y} k_d(x) \cdot (1 - \Omega_d(x))^2. \tag{6}$$

We simplify Eq. (6) in three ways. First, because precipitation and dissolution of $CaCO_3$ balance the flux of alkalinity through the ocean on ~10^4 yr timescales (Walker et al., 1981; Archer et al., 1997), we limit our model to these timescales and assume quasi-steady state ($\frac{dALK}{dt} \approx 0$). Although model solutions are not valid on timescales longer than this, the model may be applied to any individual time interval of 10^4–10^5 yrs at any time in Earth history given appropriate boundary conditions (e.g. Ca^{2+}, DIC, ALK).

Second, we group the precipitation/dissolution reactions in Eq. (6) into three terms that reflect the spatial distribution of these processes: 1) $CaCO_3$ precipitation in the surface ocean 2) $CaCO_3$ precipitation in sediments, and 3) $CaCO_3$ dissolution (in sediments). $CaCO_3$ precipitation in the surface ocean refers to sources of $CaCO_3$ that use well-mixed surface ocean seawater (Ω_s). This includes the calcifying organisms responsible for the bulk of the biogenic $CaCO_3$ in the geologic record (e.g. corals, sponges, algae, and foraminifera) as well as inorganic precipitates (e.g. whitings (Morse, 2003)) that originate above the sediment–water interface. $CaCO_3$ precipitation in sediments denotes $CaCO_3$ (inorganic or biologically mediated) that precipitates below the sediment-water interface (Ω_b). Examples include crystal fans

and inorganic cements as well as $CaCO_3$ precipitated on organic surfaces (e.g. Braissant et al., 2007) at or below the sediment–water interface.

Finally, we relate local values of Ω (Ω_s and Ω_b) to each other by assuming that Ω_b is some fraction of Ω_s ($\Omega_b = \Omega_s \cdot (1 - \Delta\Omega^*)$) where $\Delta\Omega^*$ is the Ω_s-normalized gradient in Ω $\left(\Delta\Omega^* = \frac{\Omega_s - \Omega_b}{\Omega_s}\right)$ between the site of $CaCO_3$ precipitation and burial. Each unit of $CaCO_3$ produced will be associated with a unique value of $\Delta\Omega^*$ depending on the path it takes between precipitation and burial. For example, $CaCO_3$ exported to the deep sea will be associated with a larger value of $\Delta\Omega^*$ than $CaCO_3$ buried on continental shelves due to higher $CaCO_3$ solubility in the deep sea (Millero, 1976). Importantly, when calculating values of $\Delta\Omega^*$, we consider only the upper tens of centimeters of the sediment column, where the timescale for diffusion from the overlying seawater is fast. As our model represents the global $CaCO_3$ cycle, values of $\Delta\Omega^*$ represent the average gradient in Ω traversed by the global $CaCO_3$ flux (a detailed discussion of $\Delta\Omega^*$ can be found in Section 4). These simplifications reduce Eq. (6) to:

$$W = k_{ps} \cdot (\Omega_s - 1)^2 + k_{pb} \cdot (\Omega_s \cdot (1 - \Delta\Omega^*) - 1)^2 \quad \text{if } \Omega_b \geq 1 \qquad (7a)$$

$$W = k_{ps} \cdot (\Omega_s - 1)^2 - k_d \cdot (1 - \Omega_s \cdot (1 - \Delta\Omega^*))^2 \quad \text{if } \Omega_b < 1. \qquad (7b)$$

Eq. 7a and b can be solved for Ω_s (the value of Ω in the surface ocean) given values for weathering (W), k_{ps}, k_{pb}, k_d, and $\Delta\Omega^*$. The rate constants k_{ps}, k_{pb}, and k_d incorporate all of the factors that contribute to the kinetics of the global $CaCO_3$ cycle. For example, k_{ps} is a function of the calcifying organism (e.g. corals, algae, sponges) and all of the attendant biological and environmental factors that help determine its importance in the global $CaCO_3$ cycle (e.g. nutrients, temperature/salinity, continental shelf area, etc.). Similarly, k_{pb}, and k_d will depend on the reaction rate constants for inorganic $CaCO_3$ precipitation/dissolution (Morse et al., 2007), the length scale of gradients in Ω in sediments (Martin and Sayles, 2006) as well as the mass and surface area of $CaCO_3$ available for dissolution or crystal growth. k_{pb} will also depend on catalytic surfaces that promote $CaCO_3$ nucleation (Braissant et al., 2007) as well as dissolved ions other than Ca^{2+} that inhibit $CaCO_3$ precipitation by changing mineral surface and/or solution chemistry (Morse et al., 2007 and references therein). Given the variety of factors that influence the kinetics of $CaCO_3$ precipitation and dissolution and the likelihood that these factors have changed significantly over Earth history, we explore the sensitivity of our model to a range of rate constants.

4. $\Delta\Omega^*$: the distribution of carbonate mineral saturation in the ocean and sediments

In this section, we examine the processes that control the distribution of Ω in the ocean and sediments to understand how $\Delta\Omega^*$ has changed over Earth history. As long as $[Ca^{2+}] \gg [CO_3^{2-}]$ ($\frac{[Ca^{2+}]}{[CO_3^{2-}]} = 25$ in the modern ocean), the distribution of Ω in the ocean and sediments will depend largely on gradients in CO_3^{2-} and changes in $CaCO_3$ solubility associated with variations in temperature and pressure. Gradients in CO_3^{2-} are produced by any process that changes the distribution DIC and/or alkalinity in the ocean and sediments. The most important of these is the production and respiration of organic carbon (i.e. the biological pump), a process that transports large amounts of CO_2 and alkalinity, if respiration involves S, N, Fe, or Mn reduction, from the surface ocean to the water column and sediments.

In addition to the distribution of DIC and alkalinity, gradients in Ω in the ocean and sediments will also depend on the size of the DIC reservoir (e.g. Arp, 2001). For a given gradient in DIC, the associated change in Ω will be much smaller if the size of the marine DIC reservoir is large, whereas large gradients in Ω are possible if the DIC reservoir is small (Figs. 1 and 2:C–D). The size of the marine DIC reservoir depends on the total amount of CO_2 in the ocean–atmosphere system and how it is partitioned between the ocean
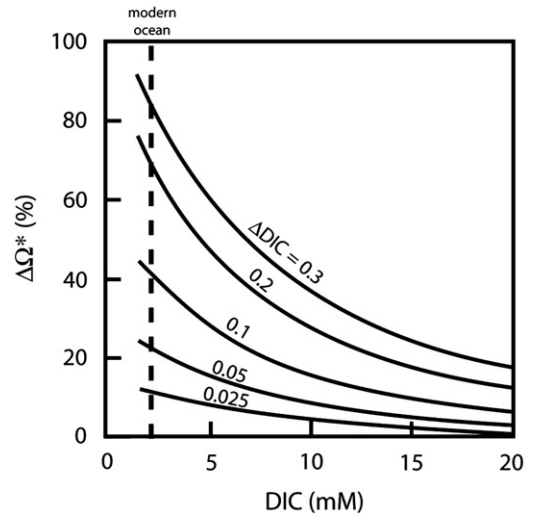
Fig. 1. Contours of ΔDIC ($DIC_1 - DIC_2$) on a plot of $\Delta\Omega^*$ $\left(\Delta\Omega^* = \frac{\Omega_1 - \Omega_2}{\Omega_1}\right)$ vs. the size of the DIC reservoir. When the DIC reservoir is small (modern ocean ≈ 2 mM), small gradients in DIC lead to large gradients in Ω (large values of $\Delta\Omega^*$). When the DIC reservoir is large, Ω is well-buffered to small ΔDIC. A ΔDIC of 0.25 is equivalent to the surface to deep ocean gradient in the Pacific ocean (Broecker and Peng, 1982).

and atmosphere. At constant pCO₂, the DIC reservoir will be large if seawater alkalinity is high. Similarly, at constant seawater alkalinity, the DIC reservoir will be large if pCO₂ is high.

4.1. Gradients in Ω due to temperature and pressure

$CaCO_3$ becomes increasingly soluble at high pressures. As a result, values of Ω in seawater will tend to decrease with depth. Given the temperature and pressure dependence of $CaCO_3$ solubility and carbonate equilibria (Millero, 1995) and assuming modern tropical surface ocean carbonate chemistry (DIC = 2.1 mM, alkalinity = 2.3 mM, $[Ca^{2+}] = 10$ mM, $T = 25$ °C, $S = 35$ psu) Ω decreases by 9%, 32%, and 53% between the surface ocean and 1, 3, and 5 kilometers water depth, respectively (Fig. 2:A). The effect of temperature is small — Ω decreases by ~5% for a 25 °C decrease in temperature.

4.2. Gradients in Ω due to carbon fixation/respiration

Changes in the distribution of CO_2 in the ocean and sediments associated with the production, transport, and remineralization of organic carbon can generate large gradients in Ω over a wide-range of lengthscales, from microns surrounding microbial filaments in surface sediments to thousands of meters in the water column. Although the effect of organic carbon cycling on Ω does not depend strongly on the length scale, different processes maintain gradients in Ω in the water column and sediments. In the water column, large-scale gradients in Ω are set by the flux of organic carbon out of the surface ocean (i.e. the strength of the biological pump). The strength of the biological pump is controlled by changes in and interactions between the global nutrient (N,P) inventory, the burial of organic carbon and nutrients, and ocean mixing (Broecker and Peng, 1982; Van Cappellen and Ingall, 1996) Although there are exceptions (see Section 4.2.2), a strong biological pump will be associated with large gradients in Ω whereas small gradients in Ω in the water column are expected when the biological pump is weak. In contrast to the water column, gradients in Ω in sedimentary pore waters reflect the balance between diffusion-limited transport of dissolved species (augmented by bioturbation at shallow depths; (Boudreau, 1987)) and the rate and distribution of organic carbon oxidation. Importantly, the slow rate of transport by diffusion (when compared to mixing in the water column) enables the development of large gradients in Ω within a short distance of the
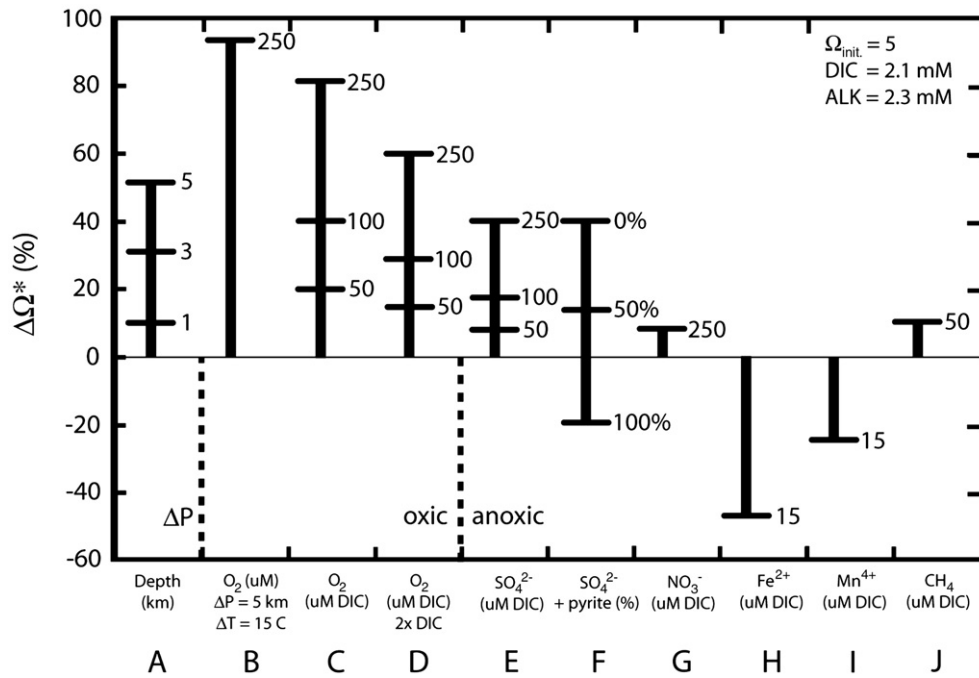
Fig. 2. Gradients in Ω ($\Delta\Omega^*$) due to the effects of pressure and temperature, oxic respiration of organic carbon, and anoxic respiration of organic carbon. A: Gradient in Ω ($\Delta\Omega^*$) between the surface ocean and 1 km, 3 km, and 5 km water depth. B: $\Delta\Omega^*$ for the modern (oxic) ocean assuming a depth change of 5 km, a temperature change of 15 °C, and a 250 μM gradient in DIC. C: $\Delta\Omega^*$ as a function of the gradient in DIC assuming oxic respiration of organic carbon (ΔALK:ΔDIC = 0). Calculated for DIC gradients of 50, 100, and 250 μM. D: The same as C except the size of the DIC reservoir is 2× (4.2 mM). E: $\Delta\Omega^*$ as a function of the gradient in DIC assuming the organic carbon is respired using sulfate (ΔALK:ΔDIC = 1). Calculated for DIC gradients of 50, 100, and 250 μM. F: Effect of pyrite precipitation on $\Delta\Omega^*$. Calculated for a DIC gradient of 250 μM assuming sulfate reduction. 0, 50, and 100% refer to the fraction of H_2S produced that is removed as pyrite. G: $\Delta\Omega^*$ as a function of the gradient in DIC for organic carbon that is respired using nitrate (ΔALK:ΔDIC = 0.8). Calculated for a DIC gradient of 250 μM. H: $\Delta\Omega^*$ as a function of the gradient in DIC for organic carbon that is respired using Fe-oxides (ΔALK:ΔDIC = 8). Calculated for a DIC gradient of 15 μM. I: $\Delta\Omega^*$ as a function of the gradient in DIC for organic carbon that is respired using Mn-oxides (ΔALK:ΔDIC = 4). Calculated for a DIC gradient of 15 μM. J: $\Delta\Omega^*$ as a function of the gradient in DIC for organic carbon that is fermented (ΔALK:ΔDIC = 0). Calculated for a DIC gradient of 50 μM.

sediment–water interface (millimeters to centimeters; (Walter and Burton, 1990; Boudreau and Canfield, 1993; Ku et al., 1999).

Gradients in Ω associated with organic carbon cycling also depend on the identity of the redox pair because the reduction/oxidation of electron donors/acceptors other that O_2/H_2O cause changes in alkalinity (e.g. SO_4^{2-}/H_2S, NO_3^-/NH_4^+, $Fe(OH)_3/Fe^{2+}$). Although there are a number of redox partners for organic carbon fixation that may have been important on the early Earth (e.g. Fe^{2+} (Walker, 1987)), for simplicity we consider only O_2/H_2O. Taking into account changes in alkalinity associated with anaerobic pathways of carbon fixation does not significantly change the results presented here. The reason for this is that high concentrations of atmospheric CO_2 and a large ocean DIC reservoir in Archean and Paleoproterozoic time would have largely suppressed gradients in Ω associated with organic carbon cycling, regardless of the pathway of fixation/respiration (see Section 6.1). Because the oxygen content of bottom waters and sediments has likely changed significantly since Archean/Proterozoic time (e.g. Canfield, 1998) we do consider the effect of organic carbon respiration under oxic and anoxic conditions.

4.2.1. $\Delta\Omega^*$ and oxic respiration

When pO₂ is high and O_2 is the dominant electron acceptor for respiration, organic carbon cycling leads to large negative gradients in Ω between the site of organic carbon production (surface ocean) and remineralization (water column and sediments). For example, a DIC gradient due to oxic respiration of 250 μM, comparable to the vertical gradient observed in the modern ocean (Broecker and Peng, 1982), will be associated with an 80% decrease in Ω between the site of production and respiration (Fig. 2). Similarly, oxic respiration of organic carbon in sediments leads to values of Ω in near-surface sedimentary pore waters that are much lower than those in the overlying seawater. When sufficient organic carbon is present, for

example in sediments on the continental shelf, slope, and rise, O_2 consumption in sediments is complete within a few millimeters to centimeters of the sediment–water interface (Cai and Sayles, 1996), and gradients in Ω in pore waters depend primarily on O_2 in bottom waters (see Fig. 2:C). O_2 may also be consumed during the oxidation of inorganic reduced species produced during anoxic remineralization (e.g. H_2S (Jorgensen and Revsbech, 1983)). The magnitude in the associated drop in Ω is slightly larger and occurs over an even shorter length scale compared to the drop in Ω due to O_2 consumption by oxic respiration (Boudreau and Canfield, 1993). Regardless of the identity of the O_2 sink, the large drop in Ω associated with O_2 consumption over such short length scales in sediments leads to undersaturation and $CaCO_3$ dissolution, even when the overlying seawater is characterized by high values of Ω (Walter and Burton, 1990; Tribble, 1993; Ku et al., 1999).

4.2.2. $\Delta\Omega^*$ and anoxic respiration

If pO₂ is low and/or the flux of organic carbon out of the surface ocean outstrips the supply of O_2 to the water column and sediments, a significant fraction of the exported organic carbon may be respired with electron acceptors other than O_2 (e.g. SO_4^{2-}, Fe(III), Mn(IV), NO_3^-). Anoxic respiration will have two effects on the distribution of Ω in the ocean and sediments. First, oceans characterized by persistent and long-term anoxia (>10^8 yrs) due to low pO₂ will be associated with a weak biological pump and small gradients in Ω (small $\Delta\Omega^*$) in the water column. Records of the carbon isotopic composition of $CaCO_3$ and organic carbon suggest that, on timescales of ~10^8 yrs, the rates of organic carbon and $CaCO_3$ burial have not varied by orders of magnitude since Archean time (Schidlowski et al., 1983; Holland, 2002; Fischer et al., 2009). As a result, the strength of the biological pump on these timescales will primarily reflect the efficiency of organic carbon burial. Because organic carbon burial is more efficient

under anoxic conditions (Hartnett et al., 1998; Hedges et al., 1999), the increasing oxygenation of the ocean and sediments since Archean time should be accompanied by a strengthening of the biological pump. This need not be true for the short-lived (10^6–10^7 yrs) episodes of widespread anoxia associated with high pO_2 in the Phanerozoic (e.g. Cretaceous ocean anoxic events), where anoxia is thought to be, in part, a consequence of enhanced biological productivity (Sarmiento et al., 1988; Hotinski et al., 2000).

Second, anoxic remineralization of organic carbon may increase alkalinity, leading to higher values of Ω compared to respiration with O_2 (Fig. 2:E–J). As a result, anoxic respiration will be associated with a more homogeneous distribution of Ω in the water column and sediments (smaller $\Delta\Omega^*$). For example, assuming a ΔDIC of 250 µM, we calculate a decrease in Ω of 40% when organic carbon is respired by SO_4^{2-} reduction, compared to a drop of 80% when respiration involves O_2 (Fig. 2:C,E). Reactions involving the products of anoxic remineralization (e.g. Fe^{2+} and H_2S) can also lead to changes in Ω. The most important of these is the precipitation of sulfide-bearing minerals, which increases Ω by removing H_2S (Fig. 2:F; Ben-Yaakov, 1973).

5. $\Delta\Omega^*$ and the global CaCO$_3$ cycle

In summary, three factors control the distribution of Ω in the ocean and sediments: the size of the ocean DIC reservoir, the pressure-dependent solubility of $CaCO_3$, and the intensity and pathway of organic carbon cycling. Large gradients in Ω (e.g. values of $\Delta\Omega^* > 80\%$) arise from a combination of high pO_2, a strong biological pump, oxic respiration of organic carbon, and efficient $CaCO_3$ transport to the deep sea. Similarly, small gradients in Ω (e.g. values of $\Delta\Omega^* < 40\%$) result from either anoxic respiration of organic carbon, a weak biological pump, or a large marine DIC reservoir. Using these two cases (large and small $\Delta\Omega^*$) as end members, we return to our model of the global $CaCO_3$ cycle (Eq. 7a–b) to consider what different values of $\Delta\Omega^*$ mean for the cycling of $CaCO_3$ in the ocean and sediments.

5.1. The global CaCO$_3$ cycle when $\Delta\Omega^*$ is large

Large values of $\Delta\Omega^*$ promote $CaCO_3$ dissolution. Therefore, $CaCO_3$ dissolution will be an important process in the global $CaCO_3$ cycle when pO_2 is high, the biological pump is strong, and organic carbon is respired with O_2 (Fig. 3a,b). For a given value of $\Delta\Omega^*$, the amount of $CaCO_3$ dissolved depends on the kinetic rate constants (k_{ps} and k_d). High values of k_{ps} and/or k_d will be associated with high rates of $CaCO_3$ dissolution whereas low rates of dissolution require small k_{ps} and k_d. Large $\Delta\Omega^*$ will also result in higher values of $CaCO_3$ saturation in the surface ocean (Ω_p) for all but highest values of k_{ps} and/or lowest values of k_d. Because the long-term rate of $CaCO_3$ burial is fixed by the alkalinity input from weathering, increased dissolution must be accompanied by higher rates of $CaCO_3$ precipitation and hence higher values of Ω in the surface ocean.

The global $CaCO_3$ cycle in the modern ocean is characterized by high values of $\Delta\Omega^*$ (80–95%), a result of oxic respiration and transport of $CaCO_3$ to the deep sea (Fig. 2:B). Observations of corrosive bottom waters (Berner, 1965; Li et al., 1969) and measurements of excess Ca^{2+} and alkalinity fluxes out of sediments indicate $CaCO_3$ undersaturation and dissolution in both shallow (Walter and Burton, 1990; Ku et al., 1999) and deep-sea (Archer et al., 1989) sediments. Estimates of $CaCO_3$ cycling in the modern ocean suggest that as much as 60–80% of annual $CaCO_3$ production is re-dissolved in the water column and sediments (Archer, 1996; Milliman and Droxler, 1996). Finally, the modern surface ocean is highly oversaturated with respect to $CaCO_3$ ($\Omega = 5$–6; (Li et al., 1969)). In the context of our model, these observations require a value of k_d that is ~50 times larger than k_{ps}. This result is qualitatively consistent with arguments that changes in the rate of $CaCO_3$ dissolution is the dominant mechanism by which the balance between weathering and $CaCO_3$ burial is maintained on
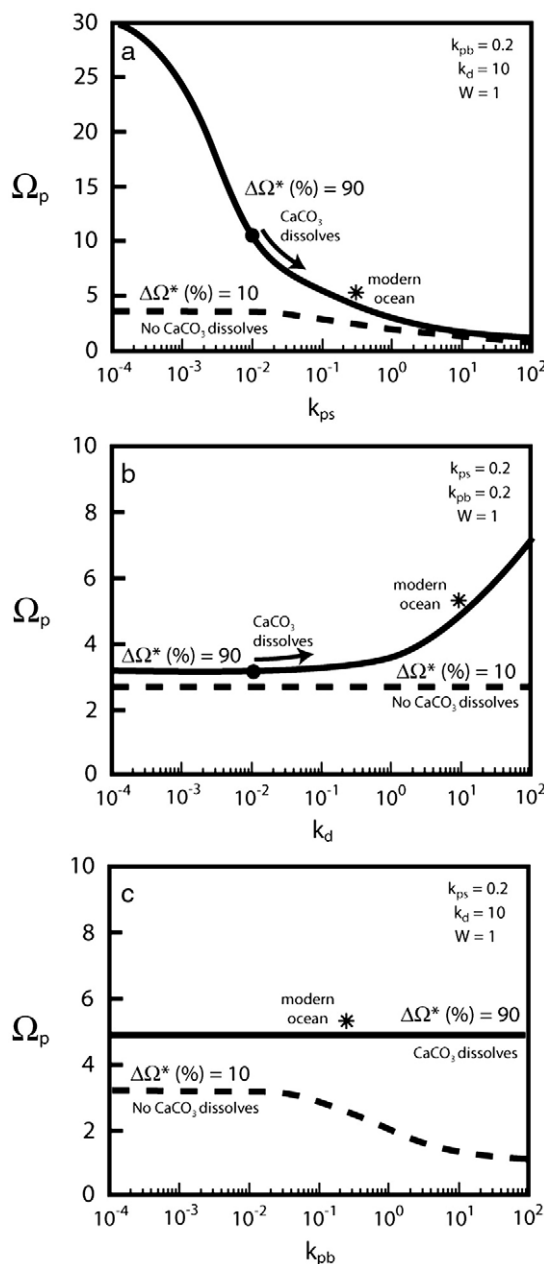
Fig. 3. a–b) Contours of $\Delta\Omega^*$ on a plot of Ω_p vs. k_{ps} and k_d (Eq. 7a,b). Large $\Delta\Omega^*$ ($\Delta\Omega^* = 90$) promotes $CaCO_3$ dissolution and supports high values of Ω_p. The amount of $CaCO_3$ dissolution increases with increasing k_{ps} and k_d. When $\Delta\Omega^*$ is small ($\Delta\Omega^* = 10$), $CaCO_3$ does not dissolve (sediments precipitate $CaCO_3$) and values of Ω_p are low. c) Contours of $\Delta\Omega^*$ on a plot of Ω_p vs. k_{pb}. Large $\Delta\Omega^*$ ($\Delta\Omega^* = 90$) suppresses $CaCO_3$ precipitation on the seafloor (promotes $CaCO_3$ dissolution). In this case, Ω_p is set only by the rate of precipitation in the surface ocean. When $\Delta\Omega^*$ is small ($\Delta\Omega^* = 10$), $CaCO_3$ precipitates in sediments. Values of Ω_p are lower than when $\Delta\Omega^*$ is large and decreases with increasing k_{pb}.

~10^4 yr timescales in the modern ocean (carbonate compensation sensu Broecker and Peng, 1982).

5.2. The global CaCO$_3$ cycle when $\Delta\Omega^*$ is small

When $\Delta\Omega^*$ is small, sediments tend to be oversaturated and may precipitate $CaCO_3$ (Fig. 3c). The partitioning of $CaCO_3$ precipitation between surface ocean and sediments depends on their respective kinetic rate constants (k_{ps} and k_{pb}). Because $CaCO_3$ dissolution is suppressed when $\Delta\Omega^*$ is small, $CaCO_3$ saturation in the surface ocean will depend only on the rate of $CaCO_3$ precipitation. Unfortunately, the

kinetics of $CaCO_3$ precipitation on the seafloor are not well understood. As a result, it is difficult to predict what value of Ω in the surface ocean will be associated with a $CaCO_3$ cycle dominated by precipitation on the seafloor.

The lack of significant inorganic precipitation in sediments overlain by supersaturated seawater in the modern ocean (Morse and Mucci, 1984) is frequently cited as evidence for slow precipitation kinetics. However, given that shallow-water sediments in the modern ocean are corrosive to $CaCO_3$ within a short distance of the sediment–water interface (Walter and Burton, 1990; Ku et al., 1999), the lack of significant inorganic precipitation in $CaCO_3$ sediments in the modern ocean may simply reflect large gradients in Ω associated with intense oxic cycling of organic carbon. Slow precipitation kinetics and high values of Ω in the surface ocean are also often inferred for Archean and Proterozoic seafloor precipitates based on hypotheses of kinetic inhibition by ions soluble in anoxic seawater (Sumner and Grotzinger, 1996b)) and comparisons with modern sedimentary precipitates (Kempe and Kazmierczak, 1990; Kempe et al., 1991). Although the composition of Precambrian seawater did include ions (e.g. Fe^{2+}) that have been shown to inhibit $CaCO_3$ precipitation (Meyer, 1984; Katz et al., 1993), the degree of inhibition depends on multiple factors (e.g. the abundance of precipitation nuclei) such that a unique precipitation rate cannot be determined from the presence of inhibitors alone. In addition, with respect to modern analogues of Precambrian seafloor precipitates, relationships between the value of Ω in the bulk solution and precipitation rates are complicated by the gradients in Ω associated with cycling of organic carbon discussed above and the fact that the value of $CaCO_3$ saturation in any lake or ocean reflects a dynamic balance between alkalinity inputs, precipitation, and dissolution (if it occurs). Thus, although most studies argue that the kinetics of $CaCO_3$ precipitation on the seafloor are slow and should be associated with extremely high values of Ω in the surface ocean, there is a large degree of uncertainty and lower values of Ω (perhaps even lower than the modern surface ocean) should also be considered. Regardless of the particular value of Ω associated with an active seafloor carbonate factory, the key point is that oceans characterized by weak gradients in Ω in the ocean and sediments (small $\Delta\Omega^*$) favor $CaCO_3$ preservation and precipitation on the seafloor.

6. Implications for the co-evolution of ocean redox, pCO$_2$, and the global CaCO$_3$ cycle over earth history

Our model of the global $CaCO_3$ cycle suggests that gradients in Ω in the ocean and sediments exert a strong control over where $CaCO_3$ is precipitated and how much of it is re-dissolved. We apply these concepts to periods in Earth history characterized by large changes in reduction–oxidation potential of the ocean–atmosphere system and/or the size of the marine DIC reservoir. These include the Proterozoic Eon over which O_2 is hypothesized to have increased from a trace gas to a major component of Earth's atmosphere and pCO_2 declined due to increasing solar luminosity, as well as episodes of short-lived (10^6–10^7 yrs), but widespread anoxia in the Phanerozoic ocean basins.

6.1. Secular trends in CaCO$_3$ precipitation on the seafloor in the Proterozoic

Studies of Precambrian carbonate rocks indicate a decline in the importance of $CaCO_3$ precipitation directly on the seafloor in continental shelf and slope environments during the Proterozoic eon (Grotzinger, 1990; Grotzinger and Knoll, 1999). Archean and early Proterozoic carbonates facies are characterized by abundant authigenic $CaCO_3$ precipitation of both inorganic and microbial origin. They are similar in many respects to Phanerozoic marine cements with the exception that they do not fill cavity voids but rather precipitate directly as sedimentary beds on the seafloor (Grotzinger and Reed, 1983; Grotzinger and James, 2000). Examples include upward-divergent aragonite crystal fans (Sumner and Grotzinger, 2000), microdigitate stromatolites (Grotzinger

and Reed, 1983), and isopachously encrusting layers of herringbone calcite. Abundant cementation, both locally and within individual stromatolitic laminae, together with $CaCO_3$ sediment mass-balance arguments suggest that in situ $CaCO_3$ precipitation was also important in Proterozoic stromatolites (Knoll and Semikhatov, 1998; Pope and Grotzinger, 2000). With the exception of Cryogenian and basal Ediacaran 'cap carbonates', both inorganic and microbial authigenic seafloor precipitates are less common in Meso and Neoproterozoic carbonate rocks. Instead, carbonate sediments at this time suggest an increase in the abundance of carbonate mud (micrite) and stromatolite accretion dominated by sediment trapping and binding (Grotzinger and Knoll, 1999). Hypotheses for the observed secular change in $CaCO_3$ facies in the Proterozoic attribute the decline in the abundance of in situ $CaCO_3$ precipitation on the seafloor to a lowering of $CaCO_3$ saturation in seawater (Grotzinger, 1990; Grotzinger and James, 2000). Explanations for the drop in $CaCO_3$ saturation include the long-term transfer of inorganic carbon from the ocean and atmosphere to the continents associated with the formation of large, stable continents in the early Proterozoic (2.5 to 2.0 Ga) and/or declining concentrations of ions in anoxic seawater that inhibit $CaCO_3$ precipitation (Grotzinger, 1990; Grotzinger and James, 2000).

Our results cast this pattern in a different light. We propose that, the observed decline in authigenic $CaCO_3$ precipitation on the seafloor in the Proterozoic may reflect an increase in $\Delta\Omega^*$ between the surface ocean and sediments associated with rising atmospheric O_2 (Canfield, 1998) and a shrinking ocean–atmosphere DIC reservoir (Bartley and Kah, 2004). Although the evolution of atmospheric O_2 throughout Proterozoic time is not well constrained, an increase from ≤ 1 ppm at the Archean–Proterozoic boundary to tens of thousands of ppm by the early Cambrian is consistent with multiple sulfur isotope measurements (Farquhar et al., 2000; Pavlov and Kasting, 2002) and the diffusive metabolic requirements of simple metazoans (Berkner and Marshall, 1965), respectively. As a result, changes in organic carbon cycling over Proterozoic time were likely characterized by an increase in respiration rates and a strengthening of the biological pump. In addition, decreasing solar luminosity over this eon (Sagan and Mullen, 1972) and the associated decline in atmospheric CO_2 would have significantly reduced the size of the ocean DIC reservoir, though this effect may have been offset somewhat by higher concentrations of Ca^{2+} in seawater. Taking into account changes in O_2 and DIC, we estimate an increase in $\Delta\Omega^*$ from
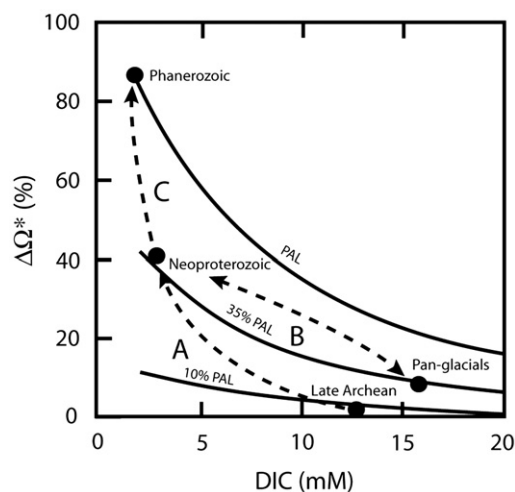

Fig. 4. Proposed changes in $\Delta\Omega^*$ over Earth history. Contours reflect different amounts of DIC respired with O_2. PAL $= 280$ μM DIC; 35% PAL $= 90$ μM DIC; 10% PAL $= 28$ μM DIC. A: $\Delta\Omega^*$ increases from the Late Archean to the Neoproterozoic due to an increase in pO_2 and a decline in the size of the seawater DIC reservoir. B: $\Delta\Omega^*$ declines significantly during Neoproterozoic pan-glacials (Hoffman et al., 1998) due to the buildup of atmospheric CO_2 and ocean DIC during glacial events. C: $\Delta\Omega^*$ increases from the Neoproterozoic to the present due to an increase in atmospheric O_2 with some contribution from the long-term drawdown in atmospheric CO_2 and the size of the DIC reservoir.

<5% to 40–50% (Fig. 4:A). Although changes in k_{ps} and k_{pb} during this interval are unconstrained, a significant decline in Ω in sediments is consistent with declining in situ precipitation of $CaCO_3$ directly on the seafloor (Grotzinger and Knoll, 1999; Grotzinger and James, 2000). In contrast to previous hypotheses where the decline in seafloor precipitation is attributed to a whole ocean decrease in $CaCO_3$ saturation (Grotzinger, 1990), our analysis suggests that the decline in Ω occurred primarily in sedimentary pore fluids. A corollary is that $CaCO_3$ saturation in the surface ocean may have actually increased through Proterozoic time.

The trend of declining precipitation on the seafloor during the Proterozoic was briefly interrupted in the aftermath of Neoproterozoic pan-glacial events (Hoffman et al., 1998). The limestone member of cap carbonate sequences that directly overlies most Neoproterozoic glacial deposits contain, in many instances, abundant seafloor precipitates including aggregates of primary aragonite fans, ranging in size from meters to decameters (Peryt et al., 1990; Grotzinger and Knoll, 1995; James et al., 2001). Current explanations for the return of seafloor precipitates following an episode of global glacial invoke high degrees of $CaCO_3$ saturation and diffusion-limited crystal growth in a post-glacial super-greenhouse (Hoffman et al., 1998; Higgins and Schrag, 2003; Shields, 2005). An alternative possibility is that the recurrence of seafloor precipitates is due to a decrease in $\Delta\Omega^*$ associated with the extremely high concentrations of DIC expected (15–20 mM; Higgins and Schrag, 2003) for an ocean equilibrated with $CaCO_3$ sediments and an atmosphere containing ~0.1 bar CO_2 (Fig. 4:B). At such high concentrations of ocean DIC, $\Delta\Omega^*$ will be small and precipitation on the seafloor favored irrespective of the oxidant or intensity of organic carbon cycling.

6.2. Implications for $CaCO_3$ cycling and ocean anoxia in the Phanerozoic

Episodes of anoxia in Phanerozoic ocean basins are distinct from those in the Precambrian in that they are less frequent, short-lived, and occur in spite of high concentrations of atmospheric O_2 (Arthur and Schlanger, 1979). Under these conditions, anoxia must result from a strengthening of the biological pump relative to the delivery of O_2 to the water column and sediments (Sarmiento et al., 1988; Hotinski et al., 2000). In contrast to anoxia in Precambrian oceans, which persisted for hundreds of millions to billions of years, anoxic events in the Phanerozoic are transient (10^6–10^7 yrs), presumably due to negative feedbacks between the burial efficiency of organic carbon and atmospheric O_2 (Van Cappellen and Ingall, 1996; Colman and Holland, 2000). Episodes of widespread anoxia in the Phanerozoic have been linked to changes in the source and/or distribution of global $CaCO_3$ production. Examples include the Late Cambrian–Early Ordovician and Permian–Triassic mass extinctions, as well as the ocean anoxic events of the Late Devonian (Frasnian–Famennian) and Cretaceous (Kiessling et al., 2002 and references therein). Although a detailed discussion of each of these events is beyond the scope of this paper, observed changes in the global $CaCO_3$ cycle during these episodes include a shift toward authigenic $CaCO_3$ precipitation on the seafloor (Grotzinger and Knoll, 1995; Copper, 2002; Pruss et al., 2006) and/or widespread drowning of carbonate platforms (Schlager, 1981 and references therein).

We propose that observed changes in the global $CaCO_3$ cycle during Phanerozoic episodes of widespread anoxia may be causally linked to a decline in $\Delta\Omega^*$ associated with an increase in the fraction of organic carbon that is respired under anoxic conditions (Fig. 2:E–J vs. C). A transient decline in $\Delta\Omega^*$ can affect the global $CaCO_3$ cycle in two ways (Fig. 5:A–B). First, if $CaCO_3$ dissolution is important, lower $\Delta\Omega^*$ will lead to more efficient $CaCO_3$ burial and a commensurate reduction in the rate of global $CaCO_3$ precipitation (Fig. 5:A). Exactly how this decline in the precipitation rate is accommodated is less clear. One possibility is that the decline in $CaCO_3$ precipitation is achieved through a reduction in the global distribution of $CaCO_3$ production. If true, this effect may help explain the relationship between widespread ocean anoxia and the
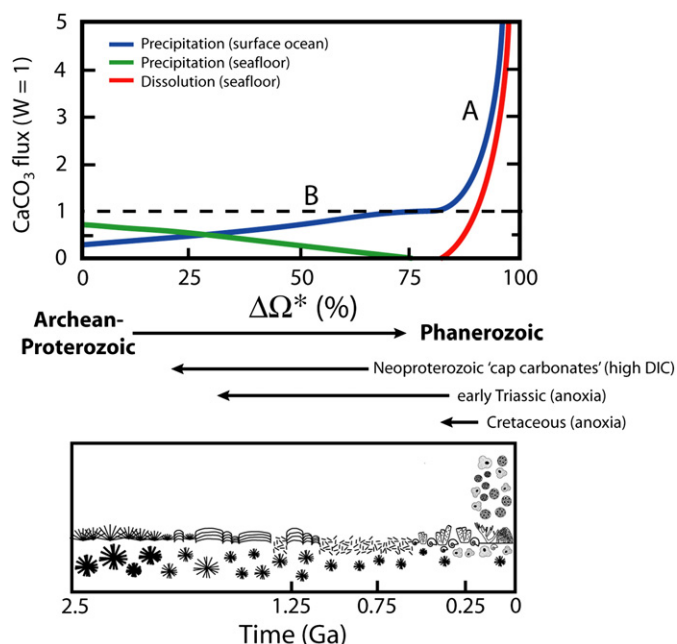
Fig. 5. Proposed changes in the global $CaCO_3$ cycle since 2.5 Ga due to the oxidation of the ocean and sediments and long-term decline in atmospheric CO_2. Upper panel depicts changes in the partitioning of the global $CaCO_3$ flux between precipitation in the surface ocean, precipitation on the seafloor, and dissolution as a function of $\Delta\Omega^*$ assuming constant k_{ps}, k_{pb}, and k_d. Bottom panel illustrates the evolution of $CaCO_3$ sediments since 2.5 Ga. A: If $CaCO_3$ dissolution is important, a decline in $\Delta\Omega^*$ must be accompanied by a decline in the rate of $CaCO_3$ precipitation so that the rate of $CaCO_3$ burial remains in balance with alkalinity inputs (W). This type of response may be consistent with observed changes in the global $CaCO_3$ cycle during Cretaceous OAEs. B: A very large drop in $\Delta\Omega^*$ will re-start the seafloor $CaCO_3$ factory at the expense of $CaCO_3$ precipitation in the surface ocean. This result could explain the return of seafloor precipitates and the delayed recovery of skeletal $CaCO_3$ producers in the early Triassic (Payne et al., 2004).

drowning of shallow-water carbonate platforms (Schlager, 1981). Second, if the drop in $\Delta\Omega^*$ is sufficiently large, authigenic $CaCO_3$ precipitation on the seafloor may occur (Fig. 5:B). Importantly, on long timescales ($>10^4$ yr), the increase in $CaCO_3$ precipitation on the seafloor must come at the expense of $CaCO_3$ precipitation in the surface ocean. This result is consistent with observations of a decline in skeletal $CaCO_3$ production and reappearance of Precambrian seafloor precipitates during periods of widespread anoxia the Phanerozoic (Grotzinger and Knoll, 1995; Copper, 2002; Kiessling et al., 2002; Pruss et al., 2006). A numerical study of oxic–anoxic transitions in a global ocean circulation–carbon cycle model (e.g. Archer and Maier Reimer, 1994) with detailed stratigraphic, sedimento-logical, and geochemical reconstructions of the changes in $CaCO_3$ cycling during anoxic events could test this aspect of our hypothesis.

7. Conclusions

Since Archean time, the concentration of atmospheric O_2 has increased by five orders of magnitude. At the same time, concentrations of atmospheric CO_2 and seawater DIC have declined by factors of 100–1000 and 5–10, respectively. We argue that these changes have had a profound effect on the global $CaCO_3$ cycle by enabling the development of large gradients in $CaCO_3$ saturation between the surface seawater and sedimentary pore fluids. Together with the evolution of $CaCO_3$ biomineralization, increasing oxic cycling of organic carbon and a reduction in atmospheric CO_2 over Earth history has led to a shift in the role of sediments in the global $CaCO_3$ cycle from a site of $CaCO_3$ precipitation to one of dissolution. Secular trends in $CaCO_3$ precipitation on the seafloor in the Precambrian and changes in the global $CaCO_3$ cycle (e.g. the return of abundant $CaCO_3$ precipitation on the seafloor and/or drowning of carbonate platforms) during episodes of widespread anoxia in Phanerozoic ocean basins may represent the response of the global

CaCO$_3$ cycle to the growth or contraction of gradients in CaCO$_3$ saturation in the ocean and sediments associated with changes in ocean–atmosphere redox and DIC.

References

Allwood, A.C., Walter, M.R., Kamber, B.S., Marshall, C.P., Burch, I.W., 2006. Stromatolite reef from the Early Archean era of Australia. Nature 441, 714–718.

Archer, D., 1996. A data-driven model of the global calcite lysocline. Glob. Biogeochem. Cycles 10, 511–526.

Archer, D., Maier Reimer, E., 1994. Effect of deep-sea sedimentary calcite preservation on atmospheric CO$_2$ concentration. Nature 367, 260–263.

Archer, D., Emerson, S., Reimers, C., 1989. Dissolution of calcite in deep-sea sediments — pH and O$_2$ microelectrode results. Geochim. Cosmochim. Acta 53, 2831–2845.

Archer, D., Kheshgi, H., MaierReimer, E., 1997. Multiple timescales for neutralization of fossil fuel CO2. Geophys. Res. Lett. 24, 405–408.

Arp, G., 2001. Photosynthesis-induced biofilm calcification and calcium concentrations in Phanerozoic oceans. Science 292, 1701–1704.

Arthur, M.A., Schlanger, S.O., 1979. Cretaceous ocean anoxic events as causal factors in the development of reef-reservoired giant oil-fields. AAPG Bull. 63, 870–885.

Bartley, J., Kah, L., 2004. Marine carbon reservoir, C$_{org}$–C$_{carb}$ coupling, and the evolution of the Proterozoic carbon cycle. Geology 32, 129.

Ben-Yaakov, S., 1973. pH buffering of pore-water of recent anoxic marine sediment. Limnol. Oceanogr. 18, 86–93.

Berkner, L.V., Marshall, L.C., 1965. On origin and rise of oxygen concentration in Earths atmosphere. J. Atmos. Sci. 22 225-&.

Berner, R.A., 1965. Activity coefficients of bicarbonate, carbonate and calcium ions in seawater. Geochim. Cosmochim. Acta 29, 947–965.

Boudreau, B.P., 1987. A steady-state diagenetic model for dissolved carbonate species and pH in the porewaters of oxic and suboxic sediments. Geochim. Cosmochim. Acta 51, 1985–1996.

Boudreau, B.P., Canfield, D.E., 1993. A comparison of close- and open-system models for porewater pH and calcite-saturation state. Geochim. Cosmochim. Acta 57, 317–334.

Braissant, O., Decho, A.W., Dupraz, C., Glunk, C., Przekop, K.M., Visscher, P.T., 2007. Exopolymeric substances of sulfate-reducing bacteria: interactions with calcium at alkaline pH and implication for formation of carbonate minerals. Geobiology 5, 401–411.

Broecker, W.S., Peng, T.H., 1982. Tracers in the Sea. Eldigio Press, Palisades, NY.

Broecker, W.S., Langdon, C., Takahashi, T., 2001. Factors controlling the rate of CaCO$_3$ precipitation on Great Bahama Bank. Glob. Biogeochem. Cycles 15, 589–596.

Burton, E.A., Walter, L.M., 1987. Relative precipitation rates of aragonite and Mg calcite from seawater — temperature or carbonate ion control. Geology 15, 111–114.

Cai, W.J., Sayles, F.L., 1996. Oxygen penetration depths and fluxes in marine sediments. Mar. Chem. 52, 123–131.

Canfield, D.E., 1998. A new model for Proterozoic ocean chemistry. Nature 396, 450–453.

Colman, A.S., Holland, D.D., 2000. The global diagenetic flux of phosphorus from marine sediments to the oceans: redox sensitivity and the ctonrol of atmospheric oxygen levels. In: Glenn, C.R., Prevot-Lucas, L., Lucas, J. (Eds.), Marine Authigenesis: From Global to Microbial. SEPM Speical Publication.

Copper, P., 2002. Reef development at the Frasnian/Famennian mass extinction boundary. Palaeogeogr. Palaeoclimatol. Palaeoecol. 181, 27–65.

Farquhar, J., Bao, H.M., Thiemens, M., 2000. Atmospheric influence of Earth's earliest sulfur cycle. Science 289, 756–758.

Fischer, W., Schroeder, S., Lacassie, J., Beukes, N., Goldberg, T., Strauss, H., Horstmann, U., Schrag, D., Knoll, A., 2009. Isotopic constraints on the late Archean carbon cycle from the Transvaal Supergroup along the western margin of the Kaapvaal Craton, South Africa. Precambrian Res. 169.

Garrels, R.M., Thompson, M.E., Siever, R., 1961. Control of carbonate solubility by carbonate complexes. Am. J. Sci. 259, 24–45.

Gattuso, J.P., Frankignoulle, M., Bourge, I., Romaine, S., Buddemeier, R.W., 1998. Effect of calcium carbonate saturation of seawater on coral calcification. Glob. Planet. Change 18, 37–46.

Grotzinger, J.P., 1990. Geochemical model for Proterozoic stromatolite decline. Am. J. Sci. 290A, 80–103.

Grotzinger, J.P., Reed, J.F., 1983. Evidence for primary aragonite precipitation, Lower Proterozoic (1.9 Ga) Rocknest Dolomite, Wopmay Orogen, Northwest Canada. Geology 11, 710–713.

Grotzinger, J.P., Knoll, A.H., 1995. Anomalous carbonate precipitates: is the Precambrian the key to the Permian? Palaios 10, 578–596.

Grotzinger, J.P., Knoll, A.H., 1999. Stromatolites in Precambrian carbonates: evolutionary mileposts or environmental dipsticks? Annu. Rev. Earth Planet. Sci. 27, 313–358.

Grotzinger, J.P., James, N.P., 2000. Precambrian carbonates: evolution of understanding. In: Grotzinger, J.P., James, N.P. (Eds.), Carbonate Sedimentation and Diagenesis in the Evolving Precambrian World. SEPM Special Publication, Tulsa, OK.

Grotzinger, J.P., Bowring, S.A., Saylor, B.Z., Kaufman, A.J., 1995. Biostratigraphic and geochronological constraints on early animal evolution. Science 270, 598–604.

Hartnett, H.E., Keil, R.G., Hedges, J.I., Devol, A.H., 1998. Influence of oxygen exposure time on organic carbon preservation in continental margin sediments. Nature 391, 572–574.

Hedges, J.I., Hu, F.S., Devol, A.H., Hartnett, H.E., Tsamakis, E., Keil, R.G., 1999. Sedimentary organic matter preservation: a test for selective degradation under oxic conditions. Am. J. Sci. 299, 529–555.

Higgins, J.A., Schrag, D.P., 2003. Aftermath of a snowball Earth. Geochem. Geophys. Geosystem 4, 20.

Hoffman, P.F., Kaufman, A.J., Halverson, G.P., Schrag, D.P., 1998. A Neoproterozoic snowball earth. Science 281, 1342–1346.

Holland, H.D., 2002. Volcanic gases, black smokers, and the Great Oxidation Event. Geochim. Cosmochim. Acta 66, 3811–3826.

Hotinski, R.M., Kump, L.R., Najjar, R.G., 2000. Opening Pandora's box: the impact of open system modeling on interpretations of anoxia. Paleoceanography 15, 267–279.

James, N.P., Narbonne, G.M., Kyser, T.K., 2001. Late Neoproterozoic cap carbonates: Mackenzie Mountains, northwestern Canada: precipitation and global glacial meltdown. Can. J. Earth Sci. 38, 1229–1262.

Jorgensen, B.B., Revsbech, N.P., 1983. Colorless sulfur bacteria, Beggiatoa spp and Thiovulum spp in O$_2$ and H$_2$S microgradients. Appl. Environ. Microbiol. 45, 1261–1270.

Kah, L.C., Grotzinger, J.P., 1992. Early Proterozoic 1.9 Ga thrombolites of the Rocknest Formation Northwest Territories Canada. Palaios 7, 305–315.

Katz, J.L., Reick, M.R., Herzog, R.E., Parsiegla, K.I., 1993. Calcite growth-inhibition by iron. Langmuir 9, 1423–1430.

Kempe, S., Kazmierczak, J., 1990. Chemistry and stromatolites of the sea-linked Satonda Crater Lake, Indonesia — a recent model from the Precambrian Sea. Chem. Geol. 81, 299–310.

Kempe, S., Kazmierczak, J., Landmann, G., Konuk, T., Reimer, A., Lipp, A., 1991. Largest known microbialites discovered in Lake Van, Turkey. Nature 349, 605–608.

Kiessling, W., Flugel, E., Golonka, J., 2002. Phanerozoic Reef Patterns SEPM Special Publication, Tulsa, OK.

Knoll, A.H., Semikhatov, M.A., 1998. The genesis and time distribution of two distinctive Proterozoic stromatolite microstructures. Palaios 13, 408–422.

Knoll, A.H., Bambach, R.K., Payne, J.L., Pruss, S., Fischer, W.W., 2007. Paleophysiology and end-Permian mass extinction. Earth Planet. Sci. Lett. 256, 295–313.

Ku, T.C.W., Walter, L.M., Coleman, M.L., Blake, R.E., Martini, A.M., 1999. Coupling between sulfur recycling and syndepositional carbonate dissolution: evidence from oxygen and sulfur isotope composition of pore water sulfate, South Florida Platform, USA. Geochim. Cosmochim. Acta 63, 2529–2546.

Langdon, C., Takahashi, T., Sweeney, C., Chipman, D., Goddard, J., Marubini, F., Aceves, H., Barnett, H., Atkinson, M.J., 2000. Effect of calcium carbonate saturation state on the calcification rate of an experimental coral reef. Glob. Biogeochem. Cycles 14, 639–654.

Li, Y.H., Takahash, T., Broecker, W.S., 1969. Degree of saturation of CaCO$_3$ in oceans. J. Geophys. Res. 74 5507-&.

Martin, J.M., Meybeck, M., 1979. Elemental mass-balance of material carried by major world rivers. Mar. Chem. 7, 173–206.

Martin, W.R., Sayles, F.L., 2006. Organic matter oxidation in deep-sea sediments: distribution in the sediment column and implications for calcite dissolution. Deep-Sea Research II 53, 771–792.

Meyer, H.J., 1984. The influence of impurities on the growth-rate of calcite. Journal of Crystal Growth 66, 639–646.

Millero, F.J., 1976. The effect of pressure on the solubility of calcite in seawater at 25 C. Geochim. Cosmochim. Acta 40, 983–985.

Millero, F.J., 1995. Thermodynamics of the carbon dioxide system in the oceans. Geochim. Cosmochim. Acta 59, 661–677.

Milliman, J.D., Droxler, A.W., 1996. Neritic and pelagic carbonate sedimentation in the marine environment: ignorance is not bliss. Geol. Rundsch. 85, 496–504.

Morse, J.W., 1978. Dissolution kinetics of calcium-carbonate in seawater: near-equilibrium dissolution kinetics of calcium carbonate-rich deep-sea sediments. Am. J. Sci. 278, 344–353.

Morse, J.W., 2003. CaCO$_3$ precipitation kinetics in waters from the great Bahama bank: implications for the relationship between bank hydrochemistry and whitings. Geochim. Cosmochim. Acta 67, 2819–2826.

Morse, J.W., Mucci, A., 1984. Composition of carbonate overgrowths produced on Iceland spar calcite crystals buried in Bahamian carbonate-rich sediments. Sediment. Geol. 40, 287–291.

Morse, J.W., Arvidson, R.S., Luttge, A., 2007. Calcium carbonate formation and dissolution. Chem. Rev. 107, 342–381.

Mucci, A., Morse, J.W., 1983. The incorporation of Mg^{2+} and Sr^{2+} into calcite overgrowths — influences of growth-rate and solution composition. Geochim. Cosmochim. Acta 47, 217–233.

Pavlov, A.A., Kasting, J.F., 2002. Mass-independent fractionation of sulfur isotopes in Archean sediments: strong evidence for an anoxic Archean atmosphere. Astrobiology 2, 27–41.

Peryt, T.M., Hoppe, A., Bechstadt, T., Koster, J., Pierre, C., Richter, D.K., 1990. Late Proterozoic aragonitic cement crusts, Bambui Group, Minas-Gerais, Brazil. Sedimentology 37, 279–286.

Pope, M.C., Grotzinger, J.P., 2000. Controls on fabric development and morphology of tufas and stromatolites, uppermost pethei group (1.8 Ga), Great Slave Lake, northwest Canada. In: Grotzinger, J.P., James, N.P. (Eds.), Carbonate Sedimentation and Diagenesis in the Evolving Precambrian World. SEPM Special Publication, Tulsa, OK.

Pruss, S.B., Bottjer, D.J., Corsetti, F.A., Baud, A., 2006. A global marine sedimentary response to the end-Permian mass extinction: examples from southern Turkey and the western United States. Earth-Sci. Rev. 78, 193–206.

Ridgwell, A., 2005. A Mid Mesozoic revolution in the regulation of ocean chemistry. Mar. Geol. 217, 339–357.

Riebesell, U., Zondervan, I., Rost, B., Tortell, P.D., Zeebe, R.E., Morel, F.M.M., 2000. Reduced calcification of marine plankton in response to increased atmospheric CO_2. Nature 407, 364–367.

Sagan, C., Mullen, G., 1972. Earth and Mars — evolution of atmospheres and surface temperatures. Science 177 52-&.

Sarmiento, J., Herbert, T., Toggweiler, J., 1988. Causes of anoxia in the world ocean. Glob. Biogeochem. Cycles 2, 115–128.

Schidlowski, M., Hayes, J.M., Kaplan, I.R., 1983. Isotopic inferences of ancient biochemistries: carbon, sulfur, hydrogen, and nitrogen. In: Schopf, J.W. (Ed.), Earth's Earliest Biosphere: Its Origin and Evolution. Princeton University Press, Princeton, N.J.

Schlager, W., 1981. The paradox of drowned reefs and carbonate platforms. Geol. Soc. Amer. Bull. 92, 197–211.

Shields, G.A., 2005. Neoproterozoic cap carbonates: a critical appraisal of existing models and the plumeworld hypothesis. Terra Nova 17, 299–310.

Stanley, S.M., Hardie, L.A., 1998. Secular oscillations in the carbonate mineralogy of reef-building and sediment-producing organisms driven by tectonically forced shifts in seawater chemistry. Palaeogeogr. Palaeoclimatol. Palaeoecol. 144, 3–19.

Sumner, D.Y., Grotzinger, J.P., 1996a. Herringbone calcite: petrography and environmental significance. J. Sediment. Res. 66, 419–429.

Sumner, D.Y., Grotzinger, J.P., 1996b. Were kinetics of Archean calcium carbonate precipitation related to oxygen concentration? Geology 24, 119–122.

Sumner, D.Y., Grotzinger, J.P., 2000. Late Archean Aragonite Precipitation: Petrography, Facies Associations, and Environmental Significance, Carbonate Sedimentation and Diagenesis in the Evolving Precambrian World. SEPM Special Publication, Tulsa, OK.

Tribble, G.W., 1993. Organic-matter oxidation and aragonite diagenesis in a coral-reef. J. Sediment. Petrol. 63, 523–527.

Urey, H.C., 1952. On the early chemical history of the Earth and the origin of life. Proc. Natl. Acad. Sci. U. S. A. 38, 351–363.

Van Cappellen, P., Ingall, E.D., 1996. Redox stabilization of the atmosphere and oceans by phosphorus-limited marine productivity. Science 271, 493–496.

Walker, J.C.G., 1987. Was the Archean biosphere upside down? Nature 329, 710–712.

Walker, J.C.G., Hays, P.B., Kasting, J.F., 1981. A Negative Feedback Mechanism for the Long-Term Stabilization of Earth's Surface-Temperature. J Geophys Res–Oc Atm, vol. 86, pp. 9776–9782.

Walter, L.M., Burton, E.A., 1990. Dissolution of recent platform carbonate sediments in marine pore fluids. Am. J. Sci. 290, 601–643.

Zeebe, R.E., Westbroek, P., 2003. A simple model for the $CaCO_3$ saturation state of the ocean: the "Strangelove", the "Neritan", and the "Cretan" Ocean. Geochem. Geophy. Geosyst. 4.

Zhong, S.J., Mucci, A., 1989. Calcite and aragonite precipitation from seawater solution of various salinities — precipitation rates and overgrowth compositions. Chem. Geol. 78, 283–299.

Zuddas, P., Mucci, A., 1998. Kinetics of calcite precipitation from seawater: II. The influence of the ionic strength. Geochim. Cosmochim. Acta 62, 757–766.